Determination of the Exchange Coupling Strengths for Fe/Au/Fe

J. Unguris, R. J. Celotta and D. T. Pierce

Electron Physics Group
National Institute of Standards and Technology
Gaithersburg, Maryland 20899

Abstract

We measure, as a function of interlayer thickness, the magnitude of the bilinear exchange coupling in an Fe/Au/Fe tri-layer, to investigate the existing order of magnitude discrepancy between theory and experiment. We use Fe whisker substrates, scanning electron microscopy with polarization analysis and reflection high energy electron diffraction to monitor the sample's magnetic and physical structure, and confocal magneto-optic Kerr effect to determine the coupling. We determine the exchange coupling strengths of the individual oscillating terms. The total bilinear coupling strength is -1.9 $\pm$ 0.2 mJ/m^2, for a Au interlayer thickness of 4 ML, in substantial agreement with current theory.

PACS numbers: 75.70.Cn, 75.70.Ak, 75.30.Pd, 75.50.Bb

It has been about a decade since experiments first revealed that two ferromagnetic layers separated by a non-ferromagnetic interlayer were, in fact, coupled [1] through an exchange mechanism that continuously reversed [2] the magnetic alignment of the ferromagnetic layers as the thickness of the non-ferromagnetic interlayer increased. Owing to many advances in theory and experiment [3,4], a much better understanding of the phenomena now exists. We now know that there may be more than one coupling oscillation period, as a function of interlayer thickness, and that these periods can be calculated from a knowledge of the interlayer Fermi surface. In experiments in which the substrate and growth conditions are stringently measured and controlled, justifying a detailed comparison with theory, excellent agreement is found between measured and predicted coupling periods. For example, for the Fe/Au/Fe(001) system, our measurements [5] of the oscillation periods, 2.48 $\pm$ 0.05 ML and 8.6 $\pm$ 0.3 ML, are in excellent agreement with the values of 2.51 ML and 8.6 ML extracted [6] from measurements of the Fermi surface.

However, there is no such agreement on the strength of the exchange coupling. In particular, for Fe/Ag/Fe(001) or Fe/Au/Fe(001), measured coupling strengths [7,8] are over an order of magnitude less than theory [9] predicts. The same discrepancy exists in other exchanged coupled systems [10]. Is current theory much better at predicting periods than amplitudes, or do the measurements simply under represent the strength of exchange coupling? The goal of this letter is to answer that question using data derived from Scanning Electron Microscopy with Polarization Analysis (SEMPA), Magneto-Optic Kerr Effect (MOKE), and Reflection High Energy Electron Diffraction (RHEED) measurements and a careful analysis of the effect of

interfacial roughness on coupling strength measurements.

To best approximate the theoretically assumed conditions by experiment, we choose to study the Fe/Au/Fe(001) system. This system is known to grow well, owing to a very close lattice match (within 0.5 %) and a favorable surface free energy ratio. Our experimental procedure consists of growing an Fe/Au/Fe(001) wedge structure *in situ* in our SEMPA microscope, confirming the existence of oscillatory coupling, overcoating with a Au passivation layer, checking that the passivation step does not affect the magnetization pattern, and finally removing the sample to a MOKE microscope to observe the change in the magnetization pattern as a function of applied magnetic field.

Single crystal Fe whiskers provide nearly ideal, well characterized [11], flat substrates with single atom steps spaced ~1 µm apart. Whiskers are cleaned by cycles of Ar-ion sputtering and annealing to 750°C. The Au is grown by molecular beam epitaxy on the Fe whisker at 100°C. The exposure is varied in order to deposit a Au wedge, the thickness of which varies continuously, typically from 0 - 10 nm over a distance of about 1 mm. Both the quality of growth and the thickness of the Au interlayer are monitored using RHEED [5]. Spatially resolved RHEED imaging permits [12] interlayer thickness measurements to an accuracy of ± 0.1 ML.

The SEMPA technique [12] uses a scanning electron microscope with a spin polarization analyzer to provide an image of surface magnetic domain structure. SEMPA simultaneously measures the two in-plane magnetization components: an x component along the whisker's long axis, and an orthogonal y component. Figure 1a is a SEMPA image of the x-component of magnetization, M_x, for the top surface of an Fe/Au/Fe wedge structure consisting of an Fe whisker substrate, a Au wedge and a 12 ML thick top Fe layer. White (black) indicates that M_x is directed in the +x (-x) direction, while gray indicates that $M_x = 0$; a similar definition applies to Fig. 1b for M_y. With no applied magnetic field the whisker is divided by a horizontal domain wall into two equivalent, but oppositely magnetized domains; for simplicity in our discussion, we will describe all of the phenomena using the lower domain. The bottom half of the image in Fig. 1a shows a pattern that oscillates between black and white, with interspersed regions of gray. Since the substrate domain is oriented in the +x, or white, direction, white regions correspond to ferromagnetic bilinear coupling, black to antiferromagnetic bilinear coupling, and gray to biquadratic or 90° coupling, which may also be clearly seen in Fig. 1b.

After confirming that the growth was good enough to replicate past SEMPA observations of coupling periods, a passivating Au overlayer was applied. Figures 1c and d show the effect of overcoating with 6 ML of Au. While the bilinear coupling oscillations appear unchanged, the relative strength of the biquadratic coupling, reflected in the transition widths, appears to be diminished, possibly as a result of changes in boundary conditions of the spin dependent quantum well.

The domain structure of the Au coated sample was measured *ex situ* in an applied magnetic field using an imaging MOKE system. The instrument we use, as seen in Fig. 2, is a 'confocal' MOKE microscope. It is an imaging instrument designed to operate at a large angle of incidence for maximum magnetic contrast and surface sensitivity. Ordinarily, in this configuration, the depth of field would limit the focused image to a single line. Therefore, to acquire an entire focused image this instrument synchronously scans both the focusing lens and a

slit aperture to allow a high dynamic range (14 bit) CCD camera to accumulate an image consisting of only in-focus line elements. The field of view is ~500 µm and resolution is ~3 µm; these are adjustable through selection of the objective lens. A ± 0.1 ML variation in Au spacer thickness occurs, due to the wedge geometry, over this resolution element.

Figure 1e shows a longitudinal MOKE image of M_x for zero applied field. Such images are produced by acquiring an image at the field of interest and subtracting an image taken at a field adequate to saturate the magnetization. Unlike SEMPA, which is sensitive to the magnetization of the top 1-2 nm of material, the MOKE technique has a sampling depth of 10 - 20 nm. Thus, Fig. 1e shows the sum of the magnetization of both the top Fe film and the whisker substrate; white (black) when both are magnetized in the +x (-x) direction, gray when they are antiparallel. Aside from sampling depth differences, the MOKE image of M_x (Fig. 1e) is identical with the SEMPA image of M_x (Fig. 1c).

Coupling strengths are measured by accumulating a series of MOKE images, similar to Fig. 1e, while varying the applied magnetic field. To increase the magnetic contrast, these images are the difference between images acquired with oppositely applied fields. Images were all taken for decreasing absolute values of the magnetic field, but since the hysteresis is small [13], the data for increasing fields are similar. Figure 3 shows a composite of 50 MOKE M_x images ordered with magnetic field increasing along the y-axis. Dark (white) regions correspond to antiparallel (parallel) alignment. Some gray regions are present due to subtle differences in the demagnetization field of the Fe whisker for oppositely directed applied magnetic fields. As the applied field increases from zero, the whisker magnetization saturates leaving an essentially single domain substrate. Approaching saturation, stray diagonal domains move along the whisker resulting in the horizontal streaks seen in Fig. 3. Following saturation, regions showing antiparallel alignment, beginning at the thickest part of the wedge, first shrink in width and finally vanish altogether.

The insert in Fig. 3 shows a typical MOKE magnetization curve for 12 layers of Au. The field at which the antiferromagnetic coupling reverses, H_{Flip}, (specifically, the field at which M has changed by 50%) is noted and used to calculate the average coupling strength, $J_{avg}(t)$, at an average Au thickness, t [14]. The use of the term average reflects the fact that some distribution of Au thickness exists in every measurement and the total coupling strength is an average of

$$J_{avg}(t) = - H_{Flip} \, t_{Fe} \, M_{Fe}$$

coupling strengths from all thicknesses present. We calculate $J_{avg}(t)$ as, where t_{Fe} is the Fe top layer thickness and M_{Fe} is the bulk Fe saturation magnetization [15]. In principle, by modeling the magnetization curve [16], one can also obtain the strength of the biquadratic coupling, but since it was relatively small and sensitive to the Au overcoat, we did not. H_{Flip} is corrected for the Fe whisker demagnetization field which, for applied fields above 11 kA/m, is estimated be 6.7 kA/m. For smaller fields, the whisker magnetization determined from the domain structure within the MOKE image field of view was used to estimate the demagnetization field. Our determination of $J_{avg}(t)$ as a function of Au thickness is shown in Fig. 4(a). The relative precision of our $J_{avg}(t)$ measurements ranges from ± 0.005 to ± 0.02 mJ/m^2 and

our average thickness, t, is accurate to $\pm$ 0.1 ML.

The measured $J_{avg}(t)$ values are noteworthy for two reasons. First, these coupling strengths are almost an order of magnitude larger than those previously measured for this system [8]. Earlier measurements were from Fe/Au/Fe tri-layers grown epitaxially on buffered GaAs substrates; the large difference in coupling strengths may be due to differences in the quality of the film growth. Second, maximum values of the coupling occur at integer Au spacer layer thicknesses. This is another indication that the growth is nearly layer-by-layer and that only a few layers contribute to $J_{avg}(t)$.

To compare the measured coupling strengths with theoretical values a model of the Au spacer layer roughness is required to relate J_n to $J_{avg}(t)$. For this purpose we fit our measured

$$ J_{avg}(t) = \sum_n \rho_n(t,w)\, J_n $$

values of $J_{avg}(t)$ with the weighted average,

$$ J_n = [\, A_1 \sin(2\pi n/\lambda_1 + \phi_1) + A_2 \sin(2\pi n/\lambda_2 + \phi_2)\,]/n^2 $$

where,

In Eq. 2, the distribution function $\rho_n(t,w)$, weights the bilinear exchange coupling strength of a single layer, J_n, by the normalized probability that the Au is n ML thick for an average Au thickness of t. The exchange coupling strength is assumed in Eq. 3 to consist of two sine waves, each with its own amplitude, period, and phase, and a common dependence on $1/n^2$. Knowledge of $\rho_n(t,w)$ and its evolution with average Au thickness, is very important to obtaining a good fit and a reliable estimate for J_n. Our approach is to represent the growth front with a Gaussian

$$ \rho_n(t,w) = \exp[-(\frac{t - n}{w(t,b,c)})^2\,]\,/\,2N, $$

function,

characterized by a width, $w(t,b,c) = c\, t^b$, and a normalization factor, N. In studies of Fe [17] and Cr [14] growth on Fe, we have found the Gaussian function and this parameterization of the width variation describe the evolution of growth very well.

We use a weighted, non-linear least squares process to fit our experimental data using Eq. 2. The parameters that determine $J_{avg}(t)$ are the amplitudes (A_1, A_2), phases (ϕ_1, ϕ_2), periods (λ_1, λ_2), and growth parameters b and c. We know the values of $\lambda_1 = 2.48 \pm 0.05$ ML and $\lambda_2 = 8.6 \pm 0.3$ ML from a previous SEMPA experiment [6]. We determine the values of growth parameters, b = 0.14 and c = 0.39, by fitting the RHEED intensity oscillations measured (before the Fe overlayer is applied) from the same sample used in the SEMPA and MOKE measurements.

We first fit the MOKE data by holding the periods and the growth parameters at the

values described above. This gives estimates for the amplitudes of $A_1 = 25.0$ mJ/(ML m)^2 and $A_2 = 3.7$ mJ/(ML m)^2. A better fit, i.e., having a lower value of chi-squared, is obtained by allowing variation of the growth parameters and, within the error limits of the prior determination [5], the periods. This fit yields $A_1 = 31.$ mJ/(ML m)^2 and $A_2 = 4.3$ mJ/(ML m)^2. The function for this best fit, which produces a very good fit over a wide range of Au thickness, is shown in Fig. 4a. The statistical error estimates for the amplitudes determined by the fitting process are $\pm$ 0.1 mJ/(ML m)^2. When the systematic errors associated with knowing the applied and demagnetization fields, the Fe top layer thickness, and the value of the Fe magnetization are considered in addition to the statistical errors, we conclude that the best estimates for the amplitudes within this model are $A_1 = 31 \pm 4$ mJ/(ML m)^2 and $A_2 = 4.3 \pm 0.5$ mJ/(ML m)^2. We also note that there is a systematic alternation of the sign of the residuals with each peak that suggests the presence of a second harmonic term.

The only theoretical estimates of the coupling strengths for this system [9] are indicated in Fig. 4b by two curves defining the envelope of the sine functions of J_n. Also plotted are our experimentally determined values for the two components of J_n, for comparison. The experimental coupling strength for the short period oscillations reaches about 60% of the theoretically predicted value, while the long period values reach about 15% of theory. This is to be contrasted with prior experimental values for the coupling strength [8] amounting to approximately 3% of those calculated for the short period. It is clear that the large disagreement between theory and experiment is greatly diminished. In fact, considering the approximate nature of the calculations, the agreement could be characterized as excellent, except for the difference between the predicted and measured long period coupling amplitudes. While small variations in the coupling strength that depend on the passivation layer thickness [18], room temperature corrections to the measurements, and the presence of other oscillatory coupling harmonics may account for some of the remaining discrepancy, it is difficult to see how these corrections could significantly change the ratio of the oscillatory coupling amplitudes.

In conclusion, we demonstrate that it is possible to determine exchange coupling strengths to a high degree of accuracy. Obtaining excellent growth conditions on very flat substrates is of key importance. Most critical is having a detailed knowledge and model of the interlayer thickness distribution. Using the parameters deduced from RHEED measurements and a non-linear fitting procedure, we determine the amplitude of individual oscillatory exchange coupling components for a structurally ideal Fe/Au/Fe system, thereby making meaningful, quantitative comparisons between theory and experiment possible.

References

1. P. Grünberg et al, Phys. Rev. Lett. **57**, 2442-45 (1986).

2. S. S. P. Parkin, N. More, K. P. Roche, Phys. Rev. Lett. **64**, 2304 (1990).

3. See for example: *Ultrathin Magnetic Structures I & II*, ed. by B. Heinrich and J. A. C. Bland, (Springer-Verlag, Berlin, 1994).

4. M. D. Stiles, Phys. Rev. **B48**, 7238 (1993); P. Bruno, Phys. Rev. **B52**, 411 (1995); D. M. Edwards et al, Mater. Sci. Eng. **B31**, 25 (1995).

5. J. Unguris, R. J. Celotta, and D. T. Pierce, J. Appl. Phys. **75**(10), 6437 (1994).

6. P. Bruno and L. Chappert, Phys. Rev. Lett. **67**, 1602 (1991).

7. Z. Celinski, B. Heinrich and J. F. Cochran, J. Appl. Phys. **73**, 5966 (1993).

8. Q. Leng et al, J. Mag. Mag. Matls. **126**, 367 (1993).

9. M. D. Stiles, J. Appl. Phys. **79**(8), 5805 (1996).

10. A. Fert and P. Bruno in Ref. 3.

11. J. A. Stroscio and D. T. Pierce, J. Vac. Sci. Technol. B **12**(3), 1783 (1994).

12. D. T. Pierce, J. Unguris, and R. J. Celotta, in *Ultrathin Magnetic Structures II*, ed. by B. Heinrich and J. A. C. Bland, (Springer-Verlag, New York, 1994) p. 117-147.

13. There is generally less than a 10% variation in the value of the field, H_{Flip}, i.e., the field where the magnetization changes by 50%, for increasing vs. decreasing fields.

14. D. T. Pierce et al, Phys. Rev. B **49**, 14564 (1994).

15. J. F. Cochran, J. Magn. Magn. Mater. **147**, 101 (1995); B. Heinrich, M. From, J. F. Cochran et al, Proc. of MRS Spring Meeting, San Francisco **313**, 119 (1993).

16. S. T. Purcell, et al, Phys. Rev. Lett. **67**, 903 (1991); W. Folkerts and S. T. Purcell, J. Mag. Mag. Matls. **111**, 306 (1992).

17. J. A. Stroscio, D. T. Pierce, and R. A. Dragoset, Phys. Rev. Lett. **70**, 3615 (1993).

18. P. Bruno, Europhys. Lett. **23**, 615 (1993); S. N. Okuno and K. Inomata, Phys. Rev. **B51**, 6139 (1995); J. J. de Vries, et al, Phys. Rev Lett. **75**, 4306 (1995).
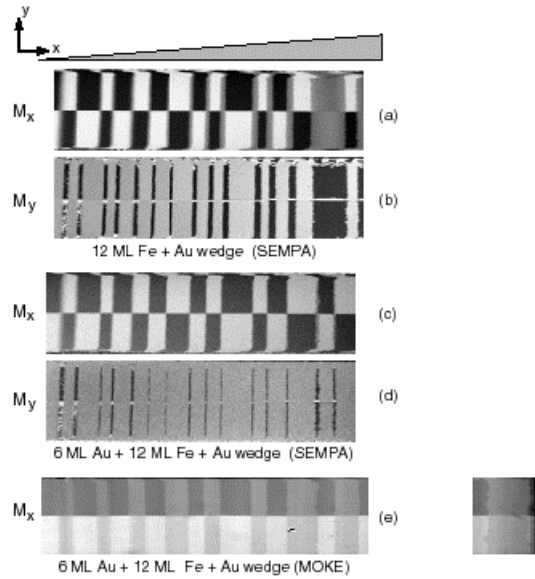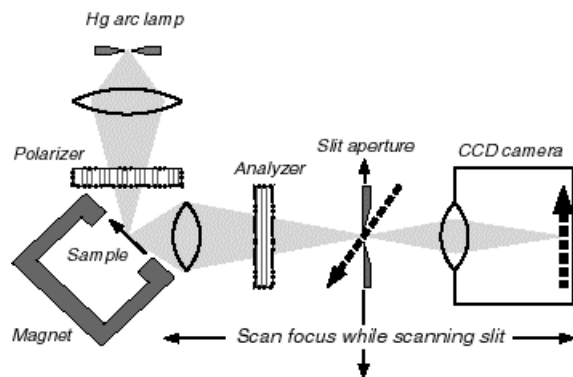
Fig. 1

1. (a) and (b) show, respectively, SEMPA measurements of the x and y components of the magnetization of the top Fe layer of the first 22 ML of a Fe/Au/Fe wedge structure. (c) and (d) show the SEMPA measurements of the same area following the addition of a 6 ML Au passivating coating. (e) shows a MOKE measurement of the x component of magnetization for the same sample used in (c) and (d).

2. A schematic diagram of the confocal MOKE microscope used in these experiments indicating the coordinated scanning of both the focus and the slit aperture.
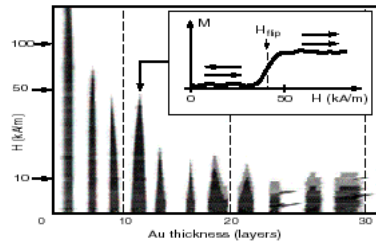
3. A collage of MOKE difference images taken as described in the text. Each image is taken at a specific applied magnetic field. The images are reduced in size vertically and placed on the (non-linear) y-axis in order of increasing magnetic field. The dark regions correspond to antiparallel coupling. Insert: Shows the magnetization curve that corresponds to a vertical cut through the fourth antiparallel coupling peak and demonstrates the selection of the H_{Flip}
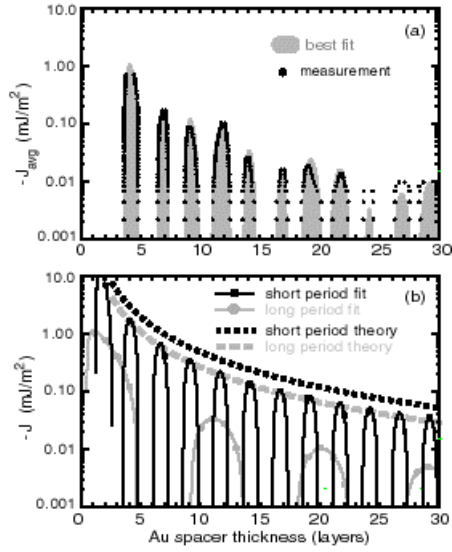
4. (a) Circles indicate the measured values of $J_{avg}(t)$ and the gray areas show the best fit function on a semi-log scale over a wide range of coupling strength and spacer layer thickness. (b) Solid squares (circles) show the variation in the short (long) period bilinear coupling strength determined by these experiments. The dark (light) dashed lines indicate the calculated maximum theoretical envelope for the short (long) period contribution to the bilinear coupling strength.